Metallic Clusters and Color Changes in Silver-Exchanged Zeolites: ^{109}Ag Solid State NMR and Optical Studies

Galina E. Pavlovskaya,*,† Charlene F. Horton-Garcia,† Cecil Dybowski,‡ David R. Corbin,§ and Thomas Meersmann†

Department of Chemistry, Colorado State University, Fort Collins, Colorado 80523, Department of Chemistry and Biochemistry, University of Delaware, Newark, Delaware 19716-2522, and Center Research and Development, DuPont Company, Wilmington, Delaware 19880-0262

Received: August 29, 2003; In Final Form: November 13, 2003

We have applied ^{109}Ag solid-state NMR and optical methods to probe dynamics and local environment of silver cations in a series of silver-exchanged zeolites as a function of hydration. In dehydrated samples of Ag−Rho, a Knight shift produced by the conduction electrons of metallic silver particles with cluster size above 400 Å is observed. Temperature dependent color change upon dehydration in zeolites Ag−X and Ag−A is also present. Although the color change in both zeolites is optically similar, NMR spectra demonstrate that fundamentally different effects lead to the color change. The color change in Ag−X zeolite is accompanied by stronger interaction of silver cations with the zeolite substrate that causes a paramagnetic contribution to the Ag shift as dehydration occurs. In Ag−A zeolite the loss of coordinated water dominates the dynamics of silver cations and leads to a more shielded Ag NMR signal upon dehydration.

Introduction

Zeolites are a class of nanostructured materials that have well-defined channels and cavities.[1] The structure of zeolites is usually composed of SiO_4^{4-} and AlO_4^{5-} tetrahedra linked at their corners to produce an anionic framework. The charge difference in zeolites is usually compensated by extraframework exchangeable cations located in the channels and cavities of zeolites. The nature of these cations usually determines catalytic and functional properties of zeolites.[2] Silver-exchanged zeolites are of particular interest because of the very nature of the Ag^+ cations. Ag^+ is the only noble monopositive cation that forms a mononuclear stable species in water. Thus, Ag^+ can be exchanged easily and completely into zeolites from aqueous solution.[3] The reversible oxidation/reduction of silver in zeolites provides a unique model system for studying mechanisms of formation of noble metal clusters within spatially well-defined zeolite channels and cavities.

Various silver zeolites are used for different purposes. Hydrated silver zeolites are light-sensitive materials and, if incorporated into membrane electrodes, they may be used to photocatalyze the decomposition of water.[4] Because quantum-size semiconductors confined in sodalite cages might be made with well defined dimensions and be uniformly distributed throughout the materials, the sodalite units provide an excellent environment for the creation of the organized assemblies of clustering species at nanometer range as potential electronic and optical materials.[3] Dehydrated brick red Ag−A zeolite has been used to detect trace amounts of moisture because the color of the material changes to orange, yellow, or white depending on the moisture content.[5] Silver mordenites are active and selective in the epoxidation of ethylene.[6] Silver-exchanged faujasites are reported to be effective catalysts for the exclusive synthesis of sialosaccharides containing specific glycosyl linkage.[7] The functional properties of silver-exchanged zeolites are strongly influenced by the position and local dynamics of silver cations. Solid-state nuclear magnetic resonance (NMR) spectroscopy is an excellent tool for probing molecular dynamics and environments of metal cations in zeolites.[8] Due to the low absolute sensitivity of both silver isotopes (^{109}Ag, 4.86×10^{-5}; ^{107}Ag, 3.43×10^{-5}) and generally long spin−lattice relaxation times, T_1, the detection of silver resonances requires extensive signal averaging. A limited number of experiments using solid-state NMR methods for the elucidation of silver behavior in nanoporous materials have been reported in the past.[9] In this study we apply solid-state ^{109}Ag spectroscopy to probe molecular dynamics and silver environment in a series of silver-exchanged zeolites as they are carried through a hydration/dehydration/rehydration cycle.

Experimental Section

Zeolites A (Aldrich), X (13X, Aldrich), Y (LZ-Y52, Linde), and mordenite (Linde M-5) were obtained commercially. Zeolite ZK-5[10] and zeolite Rho[10] were prepared using modifications of literature methods. Silver-exchanged forms of these zeolites were prepared by conventional ion-exchange techniques. Two batches of zeolites X, Y and mordenites were prepared, and one of each was calcined at 773 K. The fractional exchange in each case was estimated from elemental analysis (via ICP), as given in Table 1.

Samples were initially in the hydrated state and were examined as prepared. Dehydrated samples were prepared as follows. The material was placed in a glass tube and heated to 673 K for 22 h under a pumped pressure of 60 mTorr. In addition, four more samples were prepared from the zeolites A and X. Zeolites A and X were also dehydrated at 313 K under the vacuum, and zeolite A was also dehydrated at 473 K and 613 K under vacuum. The dehydrated samples were filled with

* Corresponding author. E-mail: galina@lamar.colosate.edu. Fax: (970)-491-1763.
† Colorado State University.
‡ University of Delaware.
§ DuPont Company.

10.1021/jp036584j CCC: $27.50
Published on Web 01/13/2004

TABLE 1: Fractional Exchange of Na by Ag and the Si/Al Ratio of Studied Materials

zeolite	Si/Al ratio	fractional ion exchange
Ag−A[a]	1.20	1.17 ± 0.03
Ag−ZK5	3.85	0.89 ± 0.03
Ag−X	1.26	0.92 ± 0.01
Ag−Y	2.74	0.85 ± 0.02
Ag−Rho (II)[b]	2.90	0.88 ± 0.09
Ag−Rho	2.80	0.59 ± 0.09
Ag−mordenite	5.1	0.77 ± 0.08

[a] The fraction of exchanged silver for Ag−A larger than 1 can be explained by the fact that when zeolite Na−A is slurried in distilled water it produces a pH of 10−10.5. This is probably due to hydrolysis of sodium ions and replacement by hydrated hydrogen ions.[11] Therefore, when Na−A is slurried in a solution containing Ag^+, some silver is precipitated as Ag_2O on the zeolite surfaces (most likely preferentially on the external surface as opposed to in the zeolite pores).[12] This hydrolysis effect is likely to be strongest in those zeolites with the lowest Si/Al ratio (the most basic materials). [b] Between two Ag−Rho samples, the material labeled II has a larger fraction of exchanged silver ion.

1 atm of molecular oxygen and were sealed in sample tubes. The presence of molecular oxygen was required to speed up the quantitative recovery of magnetization from all available silver sites in the dehydrated samples (spin−lattice relaxation times of silver in the presence of oxygen were around 3 s, as estimated by comparison of intensities of the recovered magnetization in experiments with recycle delays of 6, 10, and 20 s—no significant changes in intensities were observed for recycle delays of 10 and 20 s). UV/vis spectra were recorded from 250 to 800 nm using a Varian-Cary 4 spectrometer equipped with a Harrick diffuse-reflectance cell. Reflectance measurements were converted to absorbance data using the Kubelka−Munk relationship. NMR experiments were performed on a Chemagnetics Infinity spectrometer with a custom built probe at a nominal ^{109}Ag NMR frequency of 27.18 MHz. To minimize the effect of acoustic ringing, the data were collected with a spin−echo sequence, using spin-temperature alternation.[13] The $\pi/2$ pulse width was set to 35 μs and the echo time τ was 200 μs in all experiments. The recycle delay was set to 3 s for the hydrated samples and was increased to 10 s for the dehydrated samples to allow quantitative recovery of the magnetization. The chemical shift of a saturated aqueous $AgNO_3$ solution was used as a reference, defined to be 0 ppm.

Results

Spin−echo ^{109}Ag spectra of the materials examined in this study are shown in Figure 1. In the hydrated samples only one silver signal is detected, despite the presence of several possible cation sites for the zeolites used in this study. The absence of an observable chemical-shift difference among these sites may be the result of the fast exchange of silver cations between the sites on the NMR time scale. This is reminiscent of results previously obtained for Cd-exchanged zeolites.[14] Spectra of the hydrated zeolites are relatively narrow. The remaining broadening is probably due to residual effects from chemical-shift anisotropy and/or residual coupling to other nuclei in these materials. The estimated width did not exceed 40 ppm and in some cases (zeolite **A**) was below 20 ppm. Generally, chemical-shift anisotropies of silver in zeolites[9] are not as large as for other amphoteric metal ions such as lead[13,15] and cadmium.[14] Dehydration has a profound effect on the NMR spectra. In every case the lines become significantly broader and, in some cases, asymmetric. Most likely, the increased line widths reflect local or long-range heterogeneity of silver-cation environments in the

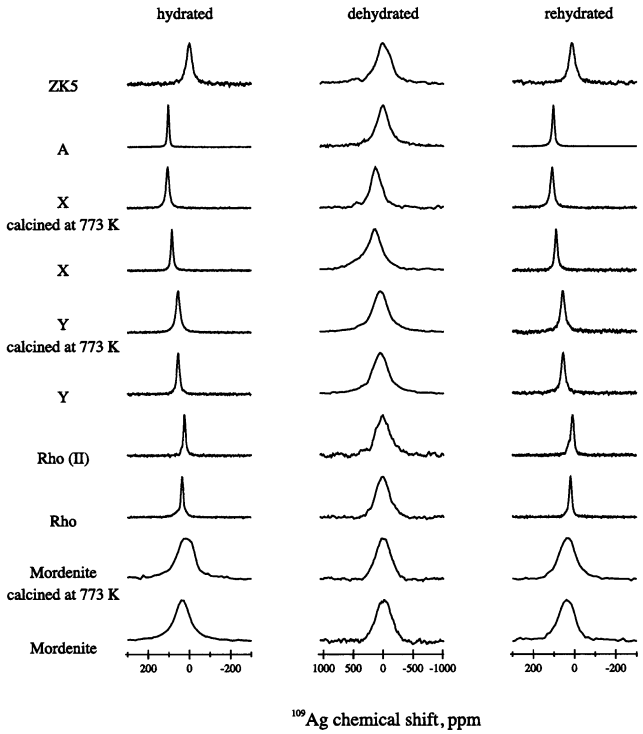

Figure 1. Spin-echo ^{109}Ag spectra of the zeolites. A Knight shift is observed for dehydrated Ag−Rho, as shown in Figure 2. Spectra of Ag−A and Ag−X are shown in more detail in Figure 5.

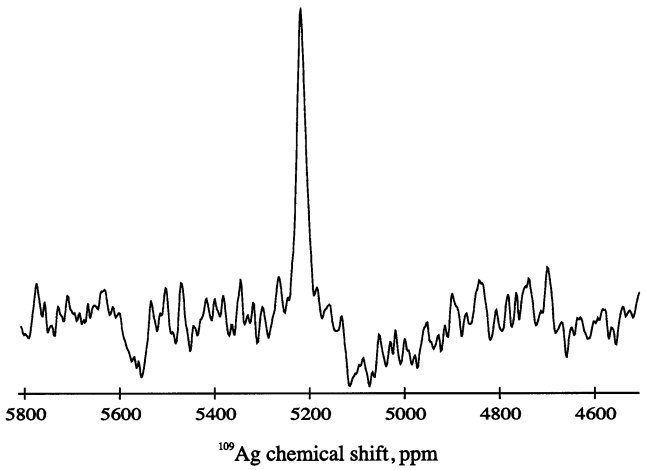

Figure 2. ^{109}Ag spectrum showing the Knight shift observed in Ag−Rho after dehydration at 773 K. The signal appears at 5220 ppm downfield from the reference. The width of the signal is 26 ppm.

dehydrated samples. We were able to detect an appreciable Knight shift of the signal in both Ag−Rho samples, Figure 2. Knight shift usually arises from interactions with the conduction electrons and its appearance in the NMR spectrum is associated with the presence of metallic particles of a size larger than 400 Å.

The exposure of the dehydrated samples to a water-rich atmosphere leads to the collapse of line widths to that of the hydrated samples. With the exception of the rehydrated Ag−Rho (both samples) the rehydrated samples also display the same chemical shifts as the original hydrated materials. The more shielded resonances of the rehydrated Ag−Rho samples (15 ppm upfield compared to the hydrated signals) indicate a lesser interaction of silver cations with the zeolite substrate (significant interactions of cations with zeolite substrate lead to the paramagnetic contribution to the chemical shift and the appear-

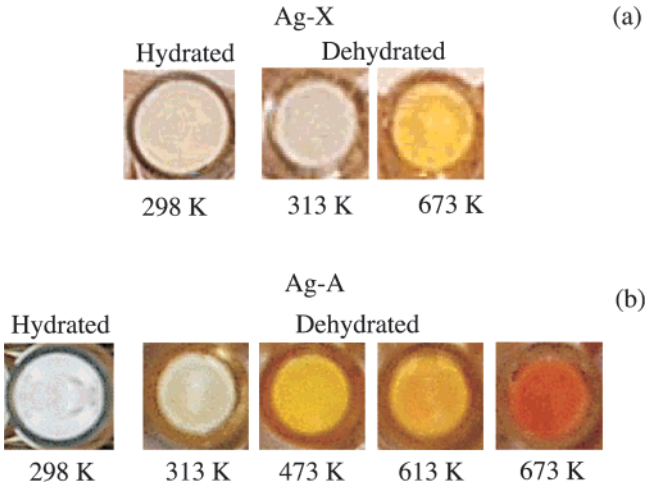

Figure 3. Color changes in zeolites in their hydration/dehydration cycle: (a) Ag−X in its hydrated and vacuum dehydrated at 313 and 673 K states; (b) Ag−A in its hydrated and vacuum dehydrated at 313, 473, 613 and 673 K states.

ance of a more deshielded signal[9]). In addition to the 15 ppm upfield shift in the rehydrated Ag−Rho samples, the signal of Ag−Rho(II) is also more broadened compared to the original hydrated material. This may be caused by parsing of silver cations into distinct sites where the exchange between the sites is slow on the NMR time scale.

Both effects are probably associated with defects induced by the formation of large metallic silver particles and their destruction upon rehydration. The absence of any observable silver signal at the Knight shift frequency in rehydrated samples supports this assumption.

Dehydration of Ag−X and Ag−A is also accompanied by a color change. Ag−X changes color from light gray to white by dehydration at 313 K and to lemon yellow at 673 K (Figure 3a). It changes back to the light gray upon the rehydration. The corresponding UV/vis spectra (Figure 4a) demonstrate the appearance of the blue band at 673 K. The NMR spectra taken in this hydration/rehydration cycle show a similar trend, as evident from Figure 5. As the dehydration occurs at 313 K the silver signal becomes broader compared to that of the hydrated sample and the resonance becomes deshielded. Dehydration at 673 K produces further broadening and deshielding accompanied by the color change. Rehydration brings the line width and the position of the signal back to those of the hydrated sample, so the process is reversible.

The color of Ag−A changes from gray to yellow and to orange depending on the dehydration temperature, as shown in Figure 3b. The UV/vis spectra acquired at each dehydration temperature show the appearance of extra bands in the blue as the dehydration temperature increases (Figure 4b). As evident from Figure 5, silver cations experience a diamagnetic shift as the dehydration temperature increases. Water exposure of samples dehydrated at any temperature leads to collapse of the line width and to the reversal of the position of the NMR signal to that of the hydrated sample. However, the color of the rehydrated Ag−A remains mustard gray and is not reversed to the original gray color upon rehydration. This can be explained by the migration of silver cations from the zeolite framework during high-temperature dehydration and subsequent formation of the reduced silver on the surface of the zeolite upon exposure to water vapors. NMR spectra show that the majority of silver cations remain inside the zeolite framework when carried

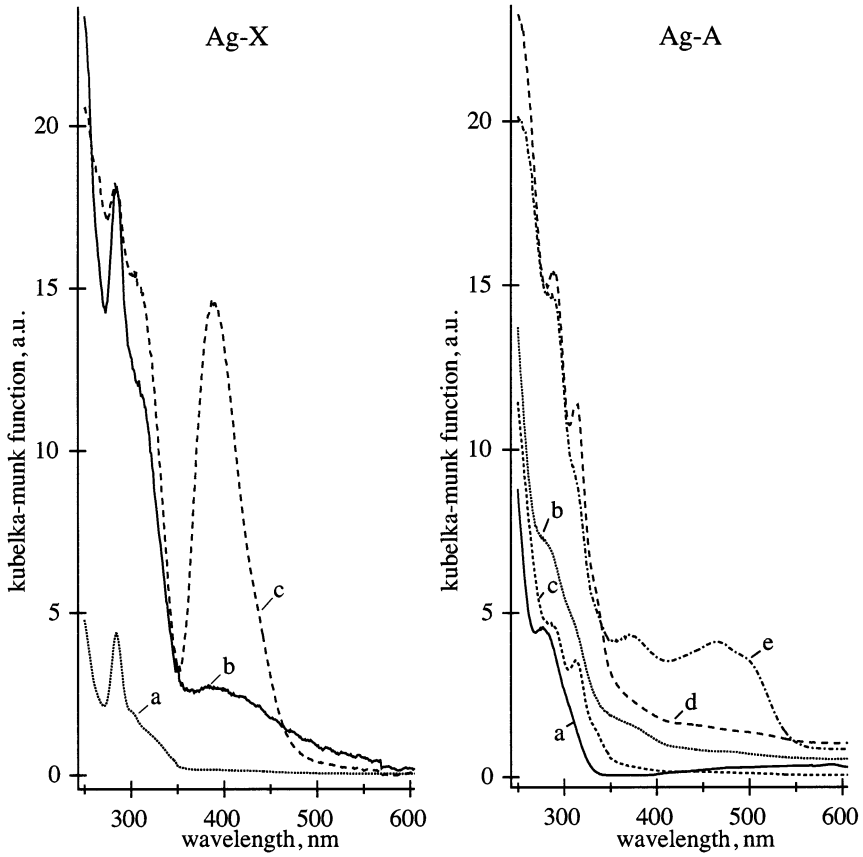

Figure 4. Uv/vis spectra of the zeolites in their hydration/dehydration cycle, illustrating the color change: Ag−X in its hydrated (a) and vacuum dehydrated at 313 K (b) and at 673 K (c) states; Ag−A in its hydrated (a) and vacuum dehydrated at 313 K (b), 473 K (c), 613 K (d), and 673 K (e) states.

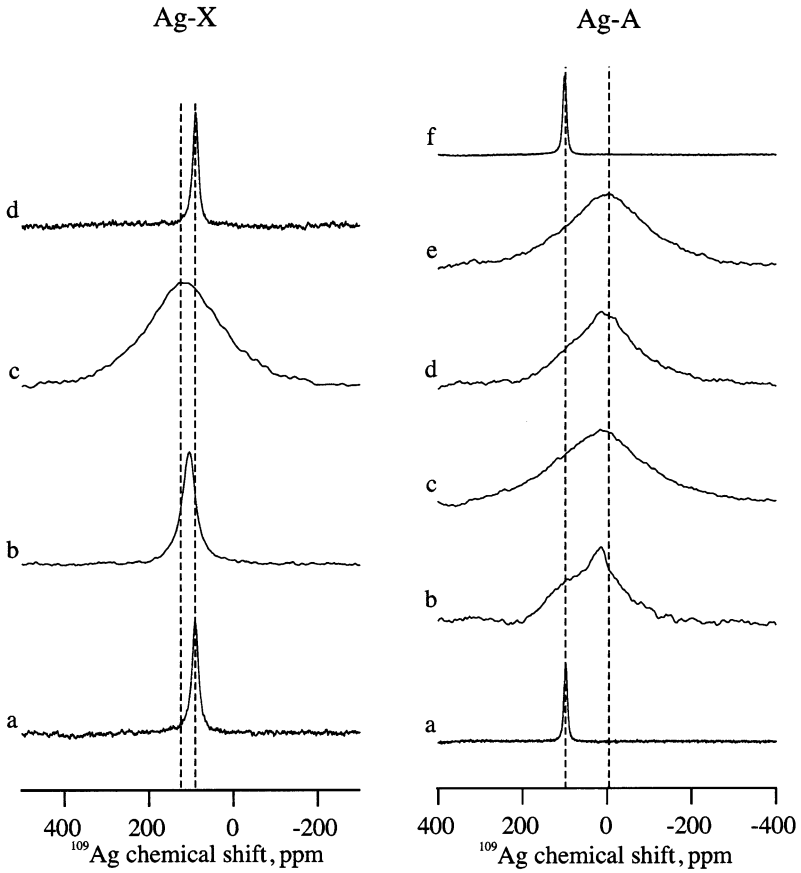

Figure 5. ^{109}Ag NMR spectra of the zeolites upon color change in their hydration−dehydration−rehydration cycle: Ag−X in its hydrated (a), vacuum dehydrated at 313 K (b) and at 673 K (c) and rehydrated (d) states; Ag−A in its hydrated (a), vacuum dehydrated at 313 K (b), 473 K (c), 613 K (d), 673 K (e), and rehydrated (f) states.

TABLE 2: Summary of Heat Treatment of Zeolites A and X and Their Chemical Shifts and Line Widths

zeolite	heat treatment	color	chemical shift, ppm	line width, ppm
	initial	grey	98	10
	313 K	beige	18	190
Ag−A	473 K	yellow	15	240
	613 K	dark yellow	10	220
	673 K	orange	−5.5	230
	rehydrated	mustard gray	100	11
Ag−X	initial	white	87	16
	313 K	white	104	38
	673 K	lemon yellow	126	219
	rehydrated	white	90	19

through the dehydration/rehydration cycle. A summary of dehydration conditions, the resulting color changes, chemical shifts and line widths for zeolites A and X are given in Table 2.

Discussion

A Knight shift was observed for both Ag−Rho samples. The structure of Ag−Rho is composed of α-cages connected by octagonal prisms forming a body-centered cubic unit cell comprising two α-cages and six octagonal prisms.[16] The structure with preferential crystallographic sites for silver cations is shown in Figure 6c. The most preferred sites are S2 in the center of a six-ring, S2*, which is displaced from the six ring into the α-cage, and the S3 site, which is displaced from a four-ring into the α-cage. $S1^1$ and $S1^2$ are sites in the octagonal prisms displaced from four-rings facing another octagonal prism or an α-cage, respectively. Zeolite Rho exhibits exceptional flexibility and its structure is particularly sensitive to temperature and hydration. It also has a negative thermal expansion upon heating. There are two temperature regions of cell contraction occurring in zeolite Rho: a rapid decrease between 298 and 348 K, and a second, more gradual decrease up to a temperature of approximately 773 K.[17] The first region corresponds to the loss of unbound water and transformation from the centric to an acentric structure, whereas the contraction in the second region is associated with the maintenance of the acentric structure.[18] This phase transformation leads to the distortion of the α-cages and to extreme mobility of extraframework cations located at S2, S2*, and S3 sites. In addition, X-ray data suggest that there are no residual water molecules in α-cages of zeolite Rho after high-temperature dehydration. Thus framework distortions induced by the phase transition and the extreme thermal mobility of Ag^+ species contribute to the autoreduction of silver in α-cages. The Ag^0 species appear to be able to migrate and aggregate on the zeolite external surface. This migration is caused by the negative charge density inside of the zeolite framework which repels the electron-rich neutral silver atoms. When reduced, the Ag^0 species also tend to interact with other Ag^0 and Ag^+ species and aggregate. If this aggregation occurs on the external surface of the zeolite then the size of the metallic species can be large enough to be detectable by NMR. This explains the appearance of the Knight shift in Ag−Rho after dehydration. However, some water molecules still remain in octagonal prisms after dehydration at 673 K.[18] Therefore, cations located at $S1^1$ and $S1^2$ sites are coordinated not only to the framework oxygens but also to water molecules. Coordination to water probably prevents autoreduction of silver, with silver

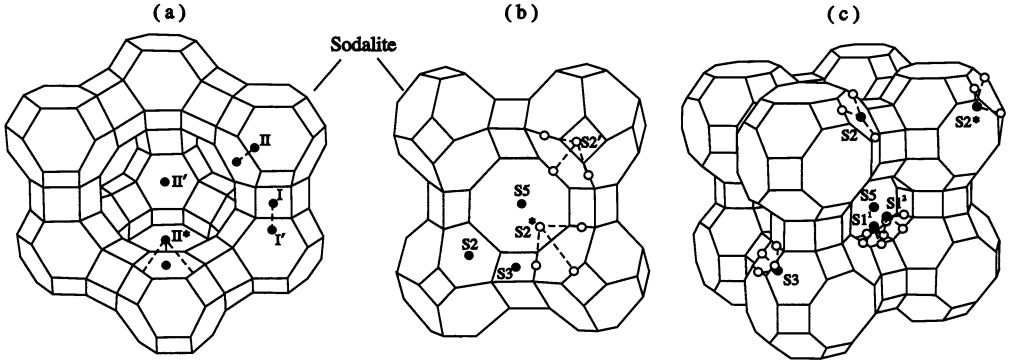

Figure 6. Structures of (a) zeolite X, (b) zeolite A, and (c) zeolite Rho showing possible cation location sites.

species located at $S1^1$ and $S1^2$ sites preserved in their cationic form. The concentration of silver cations located at these sites is sufficient to produce a strong nonmetallic NMR signal in Ag−Rho samples.

Color changes in silver-exchanged zeolites upon dehydration have previously been reported for both Ag−A[3,19,20] and Ag−X.[21] The color change in zeolite A from white to yellow was attributed to a charge-transfer interaction between Ag^+ and framework oxygens. In addition it has been suggested that, along with cationic silver coordinated to the zeolite framework, metallic silver is formed in sodalite cages of Ag−A. Further change of color from yellow to orange upon vacuum dehydration at elevated temperatures was explained by the formation of structured clusters of metallic silver acting as colored centers in the absence of water.[3] Color changes from white to yellow in Ag−X were attributed exclusively to the formation of silver clusters acting as colored centers.[21] Both materials show resonances whose position is determined by the chemical shift interaction. Knight shifts usually associated with the presence of silver particles were not observed. This result is consistent with the assumption that Ag particles must be larger than 400 Å in size to yield a Knight-shifted metallic resonance signal associated with bulk silver metal.[9] The size of metallic clusters in zeolites is usually controlled by the position of preferential adsorption of silver cations in the zeolite framework. The structures of zeolite X and zeolite A, showing possible cation location, are displayed in Figure 6. Although the structures of zeolites X and A are not the same, the fundamental building units, sodalite or β-cages, are isostructural. The major difference is that in zeolite A the sodalite cages are linked through oxygen bridges between four member rings, whereas in zeolite X the cages are bridged between six member rings forming hexagonal prisms that are big enough to place an exchangeable cation. In Ag−X, Ag^+ has a strong affinity for site I in the hexagonal prisms that join two adjacent sodalite units.[22,23] The next preferred site is I′ just outside of the hexagonal prism in the β-cage. Therefore, in zeolite X, the Ag^0 species, if formed, are trapped inside of hexagonal prisms. The trapping limits the size, migration and agglomeration of metallic species. These factors contribute to the formation of small metallic species with size much less than 400 Å. This does not lead to a detectable Knight shift in zeolite X. If the Ag^+ species are trapped inside the hexagonal prisms they are coordinated by six framework oxygens with trigonal bipyramidal symmetry.[24] The increase of the dehydration temperature induces thermal migration of the cationic species toward the zeolite framework.[21,25] As a result, the formation of a zeolite−silver complex increases the paramagnetic contribution to the chemical shift, leading to deshielding of silver cations observed with increased dehydration temperature. The lemon yellow color of Ag−X at the elevated dehydration temperature is plausibly explained by the charge-transfer interactions occurring between oxygen lone pairs of the zeolite framework and the 5s orbital of Ag^+ cations as the required spatial proximity is achieved. In Ag−A, Ag^+ prefer hexagonal window sites S2, S2*, and S2′.[26] It has been shown by xenon loading experiments that α-cages in Ag−A do not contain any charged metallic clustered species.[27] The size of neutral metallic species, if they are formed in α-cages, would be restricted by the size of an α-cage bringing the length scale of silver clusters to the regime that makes it undetectable by the solid state NMR method. Larger neutral metallic species could also form in sodalite cages. However, the size of the rigid cage also brings length constraints on the size of these metal particles, thus obscuring their detection by the NMR methods. Consequently, no NMR signal from metallic species was detected. In addition, silver cations also show a stronger affinity for coordination with water molecules. Therefore, a substantial effort is required to achieve a purely dehydrated form of this zeolite. In materials containing some water molecules, charge transfer occurs from the lone pairs of oxygens of water molecules to the Ag^+ in addition to the charge transfer from cations to the zeolite framework.[28] As silver cations lose water, they are forced to coordinate exclusively with the zeolite framework. In the absence of water, electron density is gained by cations due to charge transfer between oxygen lone pairs of the zeolite framework and the low-lying 5s orbital of silver. As a result of this increased electron density, the diamagnetic contribution to the chemical shift is increased, leading to the appearance of a more shielded NMR signal, as displayed in Figure 5. A color change from white to orange is explained by a decreased number of water ligands coordinated to the silver cation. This is consistent with previous reports that color changes in silver-containing compounds from colorless to golden yellow and brown black are accompanied by a shortening of Ag−O bonds from 2.48 to 2.51 Å to 2.05 Å, with the Ag−O bond becoming more covalent.[3]

Conclusion

We have applied ^{109}Ag solid-state NMR and optical methods to probe dynamics and local environment of silver cations in a series of exchanged zeolites carried through hydration/dehydration/rehydration cycles. We observe a chemical shift induced by the surface silver cations and a Knight shift produced by the conduction electrons of metallic silver particles in dehydrated samples of Ag−Rho. We also observed temperature-dependent color change upon dehydration in zeolites Ag−X and Ag−A. Though the color changes in these zeolites are induced by charge transfer from oxygens of the zeolite framework to the 5s orbital of silver, the electronic mechanism of this phenomenon is

different. As indicated by the NMR data, the color change in Ag−X is accompanied by stronger interaction of silver cations with the zeolite substrate and a paramagnetic chemical shift, as occurs upon dehydration. In Ag−A the loss of coordinated water dominates the dynamics of silver cations and leads to a diamagnetic chemical shift upon dehydration. Although the color change is similar, solid state ^{109}Ag NMR indicates a fundamental difference in the effects that lead to absorption in the visible range.

Acknowledgment. This material based upon work supported by the National Science Foundation Faculty Early Career Development Program under Grant No. CHE-013502.

References and Notes

(1) van Bekkum, H.; Flanigen, E. M.; Jansen, J. C. *Introduction to Zeolite Science and Technology*, 1st ed.; Elsevier: Amsterdam, 1991.

(2) Jansen, J. C.; Stocker, M.; H., K.; Weitkamp, J. *Advanced Zeolite Science and Applications*, 1st ed.; Elsevier: Amsterdam, 1994.

(3) Sun, T.; Seff, K. *Chem. Rev.* **1994**, *94*, 857.

(4) Beer, R.; Calzaferri, G.; Li, J.; Waldeck, B. *Coord. Chem. Rev.* **1991**, *111*, 193.

(5) Ralek, M.; Grubner, O.; Beyer, H.; Jiru, P. *Collect. Czech. Chem. Commun.* **1962**, *27*, 142.

(6) Jacobs, P. A.; Jaeger, N. I.; Jiru, P.; Shulz-Elkoff, C. *Metal Microstructures in Zeolites*, 1st ed.; Elsevier: Amsterdam, 1982.

(7) Thomas, R. L.; Sarkar, A. K.; Kohata, K.; Abbas, S. A.; Matta, K. L. *Tetrahedron Lett.* **1990**, *31*, 2825.

(8) Engelhardt, G.; Michel, D. *High-Resolution solid-state NMR of silicates and zeolites*, 1st ed.; John Wiley Sons Ltd.: New York, 1987.

(9) Plischke, J. K.; Benesi, A. J.; Vannice, M. A. *J. Phys. Chem.* **1992**, *96*, 3799.

(10) Robson, H. E. U.S. Patent, 1973.

(11) Breck, D. W. *Zeolite Molecular Sieves: structure, chemistry, and use*; Wiley: New York, 1973.

(12) Kragten, J. *Atlas of Metal−Ligand Equilibria in Aqueous Solution*; Halsted Press: New York, 1978.

(13) Neue, G.; Dybowski, C.; Smith, M. L.; Hepp, M.; Perry, D. L. *Solid State Nucl. Magn. Reson.* **1996**, *6*, 241.

(14) Pavlovskaya, G. E.; Ren, C. D.; Van Buskirk, M.; Dybowski, C.; Corbin, D. R.; Reimer, J. A.; Bell, A. T. *Catal. Lett.* **2002**, *80*, 19.

(15) Dybowski, C.; Smith, M. L.; Hepp, M. A.; Gaffney, E. J.; Neue, G.; Perry, D. L. *Appl. Spectrosc.* **1998**, *52*, 426.

(16) Robson, H. E.; Shoemaker, D. P.; Ogilvie, R. A.; Manor, P. C. *Adv. Chem. Ser.* **1973**, *121*, 106.

(17) Reisner, B. A.; Lee, Y.; Hanson, J. C.; Jones, G. A.; Parise, J. B.; Corbin, D. R.; Toby, B. H.; Freitag, A.; Larese, J. Z.; Kahlenberg, V. *Chem. Commun.* **2000**, 2221.

(18) Lee, Y.; Reisner, B. A.; Hanson, J. C.; Jones, G. A.; Parise, J. B.; Corbin, D. R.; Toby, B. H.; Freitag, A.; Larese, J. Z. *J. Phys. Chem. B* **2001**, *105*, 7188.

(19) Seifert, R.; Kunzmann, A.; Calzaferri, G. *Angew. Chem. Int. Ed.* **1998**, *37*, 1522.

(20) Seifert, R.; Rytz, R.; Calzaferri, G. *J. Phys. Chem.* **2000**, *104*, 7473.

(21) Hutson, N. D.; Reisner, B. A.; Yang, R. T.; Toby, B. H. *Chem. Mater.* **2000**, *12*, 3020.

(22) Aldridge, L. P.; Pope, C. G. *J. Inorg. Nucl. Chem.* **1974**, *36*, 2097.

(23) Maes, A.; Cremers, A. *J. Chem. Soc., Faraday Trans. 1* **1978**, *74*, 136.

(24) Sadlo, J.; Wasowicz, T.; Michalik, J. *Radiat. Phys. Chem.* **1995**, *45*, 909.

(25) Xu, B.; Kevan, L. *J. Phys. Chem.* **1991**, *95*, 1147.

(26) Kim, Y.; Seff, K. *J. Phys. Chem.* **1978**, *82*, 921.

(27) Moudrakovski, I. L.; Ratcliffe, C. I.; Ripmeester, J. A. *J. Am. Chem. Soc.* **1998**, *120*, 3123.

(28) Calzaferri, G.; Leiggener, C.; Glaus, S.; Schurch, D.; Kuge, K. *Chem. Soc. Rev.* **2003**, *32*, 29.